

BOUNDS PRESERVING TEMPORAL INTEGRATION METHODS FOR HYPERBOLIC CONSERVATION LAWS*

TARIK DZANIC[†], WILL TROJAK[‡], AND FREDDIE D. WITHERDEN[†]

Abstract. In this work, we present a modification of explicit Runge–Kutta temporal integration schemes that guarantees the preservation of any locally-defined quasiconvex set of bounds for the solution. These schemes operate on the basis of a bijective mapping between an admissible set of solutions and the real domain to strictly enforce bounds. Within this framework, we show that it is possible to recover a wide range of methods independently of the spatial discretization, including positivity preserving, discrete maximum principle satisfying, entropy dissipative, and invariant domain preserving schemes. Furthermore, these schemes are proven to recover the order of accuracy of the underlying Runge–Kutta method upon which they are built. The additional computational cost is the evaluation of two nonlinear mappings which generally have closed-form solutions. We show the utility of this approach in numerical experiments using a pseudospectral spatial discretization without any explicit shock capturing schemes for nonlinear hyperbolic problems with discontinuities.

Key words. Temporal integration; Runge-Kutta; Hyperbolic systems; Bounds preserving; Pseudospectral; Invariant domain preserving

AMS subject classifications. 35L65, 35L45, 65L06, 65M99

1. Introduction. This work pertains to the approximation of hyperbolic conservation laws of the form

$$(1.1) \quad \begin{cases} \partial_t \mathbf{u} + \nabla \cdot \mathbf{F}(\mathbf{u}) = 0, & \text{for } (\mathbf{x}, t) \in \Omega \times \mathbb{R}_+, \\ \mathbf{u}(\mathbf{x}, 0) = \mathbf{u}_0(\mathbf{x}), & \text{for } \mathbf{x} \in \Omega, \end{cases}$$

where d is some arbitrary space dimension, $\mathbf{u} \in \mathbb{R}^m$ is the solution, $\mathbf{F}(\mathbf{u}) \in (\mathbb{R}^m)^d$ is the flux, and $\Omega \subset \mathbb{R}^d$ is the domain. The domain is assumed to be periodic to simplify analysis with respect to the boundary conditions. We assume that there exists an admissible set of solutions to (1.1), and without giving a precise meaning to an admissible solution, which in its own right may be an open problem, we assume that there exists a well-defined set of bounds to the solution which must be satisfied to meet some criteria of admissibility. Furthermore, from Frid [3], Hoff [8], Lax [12] and related works, we assume that for general nonlinear hyperbolic systems, the notion of admissibility of these sets of solutions implies, to some extent, their convexity. As such, this motivates the development and analysis of numerical schemes in the context of their ability to satisfy convex constraints on the solution.

The literature on spatial discretizations that enforce some criteria upon the solution is vast, spanning many decades and discretization techniques [16]. However, a drawback in many of these techniques is their lack of generalizability across the various classes of spatial discretizations. By instead utilizing the method of lines approach [10], modifications to Runge–Kutta (RK) temporal integration schemes have been employed to enforce desirable criteria independently of the spatial discretization [1, 7, 9]. For more complex criteria, these approaches generally rely on some sort

*Submitted to the editors July 10th, 2021.

Funding: This work was supported by the Department of Ocean Engineering and the Department of Aerospace Engineering at Texas A&M University.

[†]Department of Ocean Engineering, Texas A&M University, College Station, TX 77843 (tdzanic@tamu.edu, fdw@tamu.edu).

[‡]Department of Aerospace Engineering, Texas A&M University, College Station, TX 77843 (wt247@tamu.edu).

of projection methods (see Hairer et al. [7] Sec. IV.4) in which the solution is projected onto a desired manifold, with various approaches effectively differing in their choices of the search direction [1, 7]. More recently, relaxation RK methods were introduced in Ketcheson [11] and shown to preserve any inner product norm by scaling the weights of the underlying RK scheme. This was extended to general convex functionals in Ranocha et al. [15] and applied to the Euler and Navier–Stokes equations with success.

In contrast to projection and relaxation methods, the objective of this work is to instead introduce a novel approach for explicit RK temporal integration schemes that guarantees the preservation of any locally-defined quasiconvex set of bounds for the solution. The proposed bounds preserving RK (BP-RK) schemes are explicit, preserve any linear invariant of the system, and recover the order of accuracy of the underlying RK schemes upon which they are built. While the applications of the proposed schemes are shown for hyperbolic conservation laws utilizing RK temporal integration, the general techniques are broadly applicable to a wider range of ordinary and partial differential equations and temporal schemes.

The remainder of this paper is organized as follows. Section 2 presents the formulations of an abstract spatial discretization and the underlying RK methods. The BP-RK schemes are introduced in Section 3, and examples of formulations of bounds are presented in Section 4. The proposed schemes are implemented and utilized on a variety of nonlinear hyperbolic systems, with implementation details given in Section 5 and results shown in Section 6. Conclusions are then drawn in Section 7.

2. Discretization. Let $\mathbf{U}_h(t) := \sum_{i \in V} \mathbf{u}_i(t) \phi_i(\mathbf{x})$ be a discrete approximation of the solution \mathbf{u} via some basis $\{\phi\}_{i \in V}$ of a finite-dimensional vector space X_h . We consider an explicit semidiscretization of (1.1) by an abstract numerical scheme given in the form of

$$(2.1) \quad \partial_t \mathbf{u}_i \approx - \sum_{j \in \mathcal{I}(i)} \mathbf{c}_{ij} \cdot \mathbf{F}(\mathbf{u}_j) = \mathbf{L}(\mathbf{u}_i, t)$$

for $i \in V$, where $\mathcal{I}(i) \subseteq V$ denotes the stencil at i and \mathbf{c}_{ij} is some \mathbb{R}^d -valued matrix dependent on the spatial discretization.

Furthermore, we consider a general explicit Runge–Kutta (RK) method of s stages represented through its Butcher tableau as

$$(2.2) \quad \begin{array}{c|c} c & A \\ \hline & b^T \end{array},$$

where $A \in \mathbb{R}^{s \times s}$ is a strictly lower-triangular matrix and $b, c \in \mathbb{R}^s$. The temporal discretization is given by

$$(2.3a) \quad \mathbf{u}_i^{n+1} = \mathbf{u}_i^n + \Delta t \sum_{k=1}^s b_k \mathbf{L}_{ik},$$

$$(2.3b) \quad \mathbf{u}_{ij}^* = \mathbf{u}_i^n + \Delta t \sum_{k=1}^s A_{jk} \mathbf{L}_{ik}, \quad j \in \{1, \dots, s\},$$

where $\mathbf{L}_{ik} = \mathbf{L}(\mathbf{u}_{ik}^*, t^n + c_k \Delta t)$, $\mathbf{u}_i^n \approx \mathbf{u}_i(t^n)$, $\mathbf{u}_i^{n+1} \approx \mathbf{u}_i(t^{n+1})$, and $t^{n+1} = t^n + \Delta t$ for some time step $\Delta t > 0$ and $n \in \mathbb{N}$.

3. Bounds Preserving Temporal Integration. Let $\mathcal{B} \subseteq \mathbb{R}^m$ be some quasi-convex, non-empty set of admissible solutions to (1.1). More generally, let there exist a unique admissible set \mathcal{B}_i for each $i \in V$. We state that the temporal integration scheme is bounds preserving if for any solution $\mathbf{u}_i^n \in \mathcal{B}_i$, there exists a sufficiently small time step $\Delta t > 0$ such that $\mathbf{u}_i^{n+1} \in \mathcal{B}_i \forall i \in V$ irrespective of the spatial discretization $\mathbf{L}(\mathbf{u}_i, t^n)$. It is clear that in their general form, the explicit RK schemes given by (2.3) are not guaranteed to be bounds preserving.

To address this, consider the mapping $\mathbf{G}_i : \mathcal{B}_i \mapsto \mathbb{R}^m$ for some $i \in V$. We define an auxiliary variable $\mathbf{w} \in \mathbb{R}^m$ such that \mathbf{G}_i is bijective with respect to \mathbf{w} , which yields the relations

$$(3.1) \quad \mathbf{w} := \mathbf{G}_i(\mathbf{u}), \quad \mathbf{u} = \mathbf{G}_i^{-1}(\mathbf{w}),$$

for some $\mathbf{u} \in \mathcal{B}_i$. If we further assume that $\mathbf{G}_i \in C^1(\mathcal{B}_i)$, then an analogous semidiscrete equation to (2.1) can be given as

$$(3.2) \quad \partial_t \mathbf{w}_i = \mathbf{G}'_i(\mathbf{u}_i) \mathbf{L}(\mathbf{u}_i, t),$$

where $\mathbf{G}'_i(\mathbf{u}_i)$ denotes the Jacobian of the mapping with respect to \mathbf{u} . We then introduce an intermediate temporal update as

$$(3.3) \quad \bar{\mathbf{u}}_i^{n+1} = \mathbf{G}_i^{-1}(\mathbf{w}_i^{n+1}) = \mathbf{G}_i^{-1} \left[\mathbf{w}_i^n + \Delta t \sum_{k=1}^s b_k \mathbf{G}'_i(\bar{\mathbf{u}}_{ik}^*) \bar{\mathbf{L}}_{ik} \right],$$

where

$$(3.4) \quad \bar{\mathbf{u}}_{ij}^* = \mathbf{G}_i^{-1} \left[\mathbf{w}_i^n + \Delta t \sum_{k=1}^s A_{jk} \mathbf{G}'_i(\bar{\mathbf{u}}_{ik}^*) \bar{\mathbf{L}}_{ik} \right]$$

and

$$(3.5) \quad \bar{\mathbf{L}}_{ik} = \mathbf{L}(\bar{\mathbf{u}}_{ik}^*, t^n + c_k \Delta t).$$

These intermediate states utilize the property that the range of $\mathbf{G}_i^{-1}(\mathbf{w})$ is \mathcal{B}_i .

LEMMA 3.1 (Bounds Preservation of the Intermediate States). *For any $i \in V$, let $\mathcal{B}_i \subseteq \mathbb{R}^m$ be some quasiconvex, non-empty set and let $\mathbf{G}_i : \mathcal{B}_i \mapsto \mathbb{R}^m$ be a bijective $C^1(\mathcal{B}_i)$ mapping. Given a solution $\mathbf{u}_i^n \in \mathcal{B}_i$, there exists a finite time step $\Delta t > 0$ such that $\bar{\mathbf{u}}_i^{n+1} \in \mathcal{B}_i$ and $\bar{\mathbf{u}}_{ij}^* \in \mathcal{B}_i$ for all $j \in \{1, \dots, s\}$ given the temporal update in (3.3) and (3.4).*

It can be seen that there exists a bijective $C^1(\mathcal{B})$ mapping \mathbf{G} for any quasiconvex, non-empty set $\mathcal{B} \subseteq \mathbb{R}^m$. As such, it is possible to construct a mapping that preserves any locally-defined quasiconvex set of bounds for the solution. The construction of these bounds and mappings is further explored in Section 4.

For any temporal integration scheme, it is essential for the scheme to at least preserve linear invariants (e.g., total mass in a periodic domain). We present the definition of linear invariant preservation through the notion of an arbitrary linear invariant residual.

DEFINITION 3.2 (Linear Invariant Residual). *Let $Q(\mathbf{u})$ be some linear invariant of \mathbf{u} (i.e., $Q(\mathbf{u}) = \mathbf{c} \cdot \mathbf{u}$, $\mathbf{c} \in \mathbb{R}^m \setminus \{\mathbf{0}\}$). The linear invariant residual is defined as*

$$(3.6) \quad R(\mathbf{u}, \mathbf{u}') = Q(\mathbf{u}) - Q(\mathbf{u}') = Q(\mathbf{u} - \mathbf{u}').$$

DEFINITION 3.3 (Linear Invariant Preservation). *Let m_i be some positive quantity dependent on the spatial discretization such that*

$$\sum_{i \in V} m_i \mathbf{u}_i^n \approx \int_{\Omega} \mathbf{U}_h(t^n).$$

The scheme is said to preserve linear invariants for a periodic domain if

$$(3.7) \quad \sum_{i \in V} m_i Q(\mathbf{u}_i^n) = \sum_{i \in V} m_i Q(\mathbf{u}_i^{n'})$$

for any linear invariant $Q(\mathbf{u})$ and $n, n' \in \mathbb{N}$, which may be identically expressed as

$$(3.8) \quad \sum_{i \in V} m_i Q(\mathbf{u}_i^n - \mathbf{u}_i^{n'}) = \sum_{i \in V} m_i R(\mathbf{u}_i^n, \mathbf{u}_i^{n'}) = 0.$$

Although the proposed intermediate temporal integration scheme is bounds preserving via the intermediate state $\bar{\mathbf{u}}_i^{n+1}$, it can be seen that it does not necessarily preserve any linear invariant of the system due to the nonlinearity of the mappings. Therefore, we define a linear invariant preserving temporal update as

$$(3.9) \quad \mathbf{u}_i^{n+1} = \bar{\mathbf{u}}_i^{n+1} + \mathbf{S}_i,$$

where $\mathbf{S}_i \in \mathbb{R}^m$ is an additional term to account for the mass defect in the intermediate states. The global mass defect is defined as

$$(3.10) \quad \bar{\mathbf{S}} := \sum_{i \in V} m_i (\mathbf{u}_i^n - \bar{\mathbf{u}}_i^{n+1}),$$

from which a component-wise unit vector can be given as

$$(3.11) \quad \mathbf{n} := \bar{\mathbf{S}} / \|\bar{\mathbf{S}}\|_2.$$

If \mathbf{S}_i is along any arbitrary unit vector, there exists a maximum vector length which can be supported such that $\bar{\mathbf{u}}_i^{n+1} + \mathbf{S}_i \in \mathcal{B}_i$. This length is formally defined by the following.

DEFINITION 3.4 (Set Distance). *For a set $X \subset \mathbb{R}^m$, the Euclidean distance from a state $\mathbf{u} \in X$ to the boundary of the set, ∂X , along some unit vector $\mathbf{n} \in \mathbb{B}^{m-1}(\mathbf{0}, 1)$ is defined as*

$$(3.12) \quad D_X(\mathbf{u}, \mathbf{n}) = \arg \min_{\gamma \geq 0} \left(\inf_{\mathbf{x} \in \partial X} \|\mathbf{u} + \gamma \mathbf{n} - \mathbf{x}\|_2 \right).$$

Along the \mathbf{n} direction, this maximum length is defined as

$$(3.13) \quad \gamma_i^* := D_{\mathcal{B}_i}(\bar{\mathbf{u}}_i^{n+1}, \mathbf{n}).$$

By setting \mathbf{S}_i as

$$(3.14) \quad \mathbf{S}_i = \gamma_i \mathbf{n}_i,$$

it can be seen from Definition 3.4 that for any $\gamma_i \in [0, \gamma_i^*]$, $\mathbf{u}_i^{n+1} = \bar{\mathbf{u}}_i^{n+1} + \mathbf{S}_i \in \mathcal{B}_i$. We therefore set γ_i as

$$(3.15) \quad \gamma_i = \gamma_i^* \|\bar{\mathbf{S}}\|_2 / \sum_{j \in V} m_j \gamma_j^*.$$

With this formulation, we now move on to state and prove the properties of the proposed schemes. The subsequent theorems utilize the following assumptions:

1. There exists a quasiconvex, non-empty set $\mathcal{B}_i \subseteq \mathbb{R}^m \forall i \in V$ such that $\mathbf{u}_i^n \in \mathcal{B}_i \forall i \in V$.
2. There exists a bijective $C^\infty(\mathcal{B}_i)$ mapping, $\mathbf{G}_i : \mathcal{B}_i \mapsto \mathbb{R}^m$, such that the intermediate temporal update defined by (3.3) results in $\bar{\mathbf{u}}_i^{n+1} \in \mathcal{B}_i \forall i \in V$.
3. Periodic boundary conditions are enforced (i.e., Ω is a d -torus).
4. The underlying spatial discretization $\mathbf{L}(\mathbf{u}, t)$ preserves linear invariants (i.e., $\sum_{i \in V} m_i \mathbf{L}(\mathbf{u}_i, t) = \mathbf{0}$).

THEOREM 3.5 (Convergence). *The temporal integration scheme defined by (3.3), (3.4), and (3.9) converges at the rate of the base RK scheme defined in (2.3).*

Proof. Let $p \geq 1$ be the order of convergence of the base RK scheme defined in (2.3) such that for the auxiliary system defined by (3.2), the relation

$$(3.16) \quad \mathbf{w}_i^{n+1} - \mathbf{w}_i^n = \Delta t \sum_{k=1}^s b_k \mathbf{T}_k = \int_{t^n}^{t^{n+1}} \partial_t \mathbf{w}_i(\tau) d\tau + \mathcal{O}(\Delta t^{p+1})$$

holds for any $i \in V$, where

$$\mathbf{T}_k = \mathbf{G}'_i(\bar{\mathbf{u}}_{ik}^*) \bar{\mathbf{L}}_{ik}.$$

The error estimate for the temporal integration scheme defined by (3.3), (3.4), and (3.9) can be given as

$$(3.17) \quad \mathbf{u}^{n+1} - \mathbf{u}^n = \mathbf{G}^{-1}(\mathbf{w}^n + \Delta t \sum_{k=1}^s b_k \mathbf{T}_k) - \mathbf{G}^{-1}(\mathbf{w}^n) + \mathbf{S}.$$

Note that the subscript is dropped for brevity. The Taylor series of $\mathbf{H}(\mathbf{w}) = \mathbf{G}^{-1}(\mathbf{w})$ can be expanded around $\mathbf{w} = \mathbf{w}^n$ and evaluated at $\mathbf{w} = \mathbf{w}^n + \Delta t \sum_{k=1}^s b_k \mathbf{T}_k$ to yield

$$(3.18) \quad \mathbf{G}^{-1}(\mathbf{w}^n + \Delta t \sum_{k=1}^s b_k \mathbf{T}_k) = \mathbf{H}(\mathbf{w}^n) + \sum_{k=1}^{\infty} \frac{1}{k!} \mathbf{H}^{(k)}(\mathbf{w}^n) \left(\Delta t \sum_{j=1}^s b_j \mathbf{T}_j \right)^k.$$

From assumption 2, the higher-order terms are well-defined as $\mathbf{G}(\mathbf{u}) \in C^\infty(\mathcal{B})$. This may be substituted into (3.17) to give

$$(3.19) \quad \mathbf{u}^{n+1} - \mathbf{u}^n = \sum_{k=1}^{\infty} \frac{1}{k!} \mathbf{H}^{(k)}(\mathbf{w}^n) \left(\Delta t \sum_{j=1}^s b_j \mathbf{T}_j \right)^k + \mathbf{S}.$$

From Ranocha et al. [15] (Theorem 2.12 with $\psi = \mathbf{H}(\mathbf{w}, t)$), this expansion is accurate to the equivalent order due to the required accuracy of the underlying RK method as a quadrature rule.

$$(3.20) \quad \sum_{k=1}^{\infty} \frac{1}{k!} \mathbf{H}^{(k)}(\mathbf{w}^n) \left(\Delta t \sum_{j=1}^s b_j \mathbf{T}_j \right)^k = \int_{t^n}^{t^{n+1}} \partial_t \mathbf{u}_i(\tau) d\tau + \mathcal{O}(\Delta t^{p+1}).$$

It now remains to be shown that $\mathbf{S} \approx \mathcal{O}(\Delta t^{p+1})$. For some arbitrary $i \in V$, this term may be expressed as

$$(3.21) \quad \mathbf{S} = \mathbf{S}_i = \zeta_i \sum_{j \in V} m_j (\mathbf{u}_i^n - \bar{\mathbf{u}}_i^{n+1}) = \zeta_i \sum_{j \in V} m_j (\mathbf{u}_i^n - \mathbf{G}^{-1}(\mathbf{w}_i^{n+1})),$$

where $\zeta_i = \gamma_i^* / \sum_{j \in V} m_j \gamma_j^*$. Utilizing the fact that m_j and ζ_i are independent of Δt and that $-(\mathbf{u}_i^n - \mathbf{G}^{-1}(\mathbf{w}_i^{n+1}))$ is identical to (3.19) with $\mathbf{S}_i = 0$, it follows that

$$(3.22) \quad \begin{aligned} \mathbf{S}_i &= -\zeta_i \sum_{j \in V} m_j \left[\int_{t^n}^{t^{n+1}} \partial_t \mathbf{u}_j(\tau) \, d\tau \right] + \mathcal{O}(\Delta t^{p+1}) \\ &= -\zeta_i \int_{t^n}^{t^{n+1}} \sum_{j \in V} m_j \partial_t \mathbf{u}_j(\tau) \, d\tau + \mathcal{O}(\Delta t^{p+1}) = \mathcal{O}(\Delta t^{p+1}) \end{aligned}$$

under the assumption that $\mathbf{L}(\mathbf{u}_j, t)$ is a consistent approximation of $\partial_t \mathbf{u}_j(t)$. As a result, we obtain

$$(3.23) \quad \mathbf{u}^{n+1} - \mathbf{u}^n = \int_{t^n}^{t^{n+1}} \partial_t \mathbf{u}(\tau) \, d\tau + \mathcal{O}(\Delta t^{p+1}). \quad \square$$

COROLLARY 3.6 (Consistency). *From Theorem 3.5, the temporal integration scheme defined by (3.3), (3.4), and (3.9) is consistent in the sense that*

$$\lim_{\Delta t \rightarrow 0} \frac{\mathbf{u}_i^{n+1} - \mathbf{u}_i^n}{\Delta t} = \frac{\partial \mathbf{u}_i^n}{\partial t}$$

for any $i \in V$.

THEOREM 3.7 (Linear Invariant Preservation). *The temporal scheme defined by (3.3), (3.4), and (3.9) preserves any linear invariant $Q(\mathbf{u})$.*

Proof. For global linear invariant preservation, it is necessary that

$$\sum_{i \in V} m_i R(\mathbf{u}_i^{n+1}, \mathbf{u}_i^n) = \sum_{i \in V} m_i Q(\mathbf{u}_i^{n+1} - \mathbf{u}_i^n) = 0,$$

which can be equivalently expressed as

$$Q(\bar{\mathbf{S}}) - \sum_{i \in V} m_i Q(\mathbf{S}_i) = 0.$$

The conclusion follows readily from the definition of \mathbf{S}_i .

$$(3.24) \quad \sum_{i \in V} m_i Q(\mathbf{S}_i) = Q\left(\sum_{i \in V} m_i \gamma_i^* \bar{\mathbf{S}} / \sum_{j \in V} m_j \gamma_j^*\right) = Q(\bar{\mathbf{S}}). \quad \square$$

Remark 3.8 (Boundary Contributions). The proof of Theorem 3.7 is contingent on the assumption that periodic boundary conditions are enforced. It is trivial to extend the definition of \mathbf{S}_i and the subsequent proof of linear invariant preservation to non-periodic domains with boundary contributions. However, this requires some dependency on the spatial discretization and does place some restriction on the formulation of the bounds as they must be able to support the boundary contributions.

THEOREM 3.9 (Bounds Preservation). *The temporal scheme defined by (3.3), (3.4), and (3.9) is bounds preserving for all $\{\mathcal{B}_i\}_{i \in V}$.*

Proof. The temporal scheme defined by (3.3), (3.4), and (3.9) is bounds preserving if

$$(3.25) \quad \mathbf{u}_i^{n+1} = \bar{\mathbf{u}}_i^{n+1} + \mathbf{S}_i \in \mathcal{B}_i \quad \forall i \in V.$$

From (3.14) and (3.15), this condition is satisfied if

$$(3.26) \quad \mathbf{S}_i = \gamma_i^* \bar{\mathbf{S}} / \sum_{j \in V} m_j \gamma_j^* \leq \gamma_i^* \mathbf{n}_i = \gamma_i^* \bar{\mathbf{S}} / \|\bar{\mathbf{S}}\|_2,$$

which may be expressed as

$$(3.27) \quad \sum_{j \in V} m_j \gamma_j^* \geq \|\bar{\mathbf{S}}\|_2.$$

Here, we switch the index from j to i for consistency with the general notation. Using $\mathbf{n} = \bar{\mathbf{S}} / \|\bar{\mathbf{S}}\|_2$ and

$$(3.28) \quad \sum_{i \in V} m_i \gamma_i^* = \left\| \sum_{i \in V} m_i \gamma_i^* \mathbf{n} \right\|_2,$$

it is sufficient to show that

$$(3.29) \quad \left(\bar{\mathbf{S}} - \sum_{i \in V} m_i \gamma_i^* \mathbf{n} \right) \cdot \mathbf{n} \leq 0.$$

From (3.10), we get

$$(3.30) \quad \left(\bar{\mathbf{S}} - \sum_{i \in V} m_i \gamma_i^* \mathbf{n} \right) \cdot \mathbf{n} = \left(\sum_{i \in V} m_i (\mathbf{u}_i^n - \bar{\mathbf{u}}_i^{n+1} - \gamma_i^* \mathbf{n}) \right) \cdot \mathbf{n},$$

from which we obtain a sufficient condition

$$(3.31) \quad \mathbf{n} \cdot (\mathbf{u}_i^n - \bar{\mathbf{u}}_i^{n+1}) \leq \gamma_i^* \quad \forall i \in V.$$

The left-hand side attains its maximum value when

$$(3.32) \quad \mathbf{u}_i^n - \bar{\mathbf{u}}_i^{n+1} = \mathbf{n} \|\mathbf{u}_i^n - \bar{\mathbf{u}}_i^{n+1}\|_2,$$

which is equivalent to

$$(3.33) \quad \mathbf{u}_i^n = \bar{\mathbf{u}}_i^{n+1} + \mathbf{n} \|\mathbf{u}_i^n - \bar{\mathbf{u}}_i^{n+1}\|_2.$$

Given that $\mathbf{u}_i^n \in \mathcal{B}_i$, from Definition 3.4, it can be seen that

$$(3.34) \quad \|\mathbf{u}_i^n - \bar{\mathbf{u}}_i^{n+1}\|_2 \leq \gamma_i^*.$$

Therefore, we obtain

$$(3.35) \quad \mathbf{n} \cdot (\mathbf{u}_i^n - \bar{\mathbf{u}}_i^{n+1}) \leq \|\mathbf{u}_i^n - \bar{\mathbf{u}}_i^{n+1}\|_2 \leq \gamma_i^*. \quad \square$$

4. Formulations for Mappings and Bounds. The choice of the mapping function $\mathbf{G}(\mathbf{u})$ dictates the properties of the proposed temporal integration schemes. In this section, we present some general mapping functions for various constraints that are of interest in numerical schemes as well as some examples of bounds for hyperbolic conservation laws.

4.1. General Mappings. For an arbitrary one-sided constraint on a scalar variable u such that $u \geq a$ for any $a \in \mathbb{R}$, the admissible set is defined as

$$(4.1) \quad \mathcal{B}(u) := [a, \infty).$$

A similar bound for $u \leq a$ may be formed by considering a sign change in u . One such example of a bijective mapping function that satisfies the condition $G^{-1}(w) \in \mathcal{B}$ is

$$(4.2) \quad G(u) = \log(u - a), \quad G^{-1}(w) = \exp(w) + a.$$

For a two-sided constraint (i.e., $a \leq u \leq b$, $a, b \in \mathbb{R}$, $b > a$), the admissible set is defined as

$$(4.3) \quad \mathcal{B}(u) := [a, b],$$

for which a mapping function can be given by

$$(4.4) \quad G(u) = \tanh^{-1}\left(2\frac{u-a}{b-a} + 1\right), \quad G^{-1}(w) = \frac{a+b}{2} + \frac{b-a}{2}\tanh(w).$$

For a vector-valued solution $\mathbf{u} \in \mathbb{R}^m$, a constraint that is of particular use for hyperbolic conservation laws is given by

$$(4.5) \quad \mathcal{B}(\mathbf{u}) := \{\mathbf{u} \mid \|\mathbf{u}\|_2 \leq r_0\}$$

for some $r_0 > 0$, which enforces the condition that the solution (or some subset thereof) exists in a closed m -ball of radius r_0 . This mapping is realized through an intermediary mapping, $\mathbf{F} : \mathcal{B} \rightarrow \mathcal{Z}$, which maps the m -ball to an m -cube, after which the mapping $\mathcal{Z} \rightarrow \mathbb{R}^m$ can be formulated as m independent two-sided scalar constraints. Various approaches exist that satisfy the necessary conditions of the intermediary mapping, from elliptic mapping to Schwarz-Christoffel conformal mapping. An example of a mapping for $m = 2$ using an elliptic approach is given as

$$(4.6) \quad \mathbf{F} \begin{pmatrix} u_1 \\ u_2 \end{pmatrix} = \begin{pmatrix} \frac{1}{2}\sqrt{2 + \delta\mathbf{u} + 2\sqrt{2}\left(\frac{u_1}{r_0}\right)} - \frac{1}{2}\sqrt{2 + \delta\mathbf{u} - 2\sqrt{2}\left(\frac{u_1}{r_0}\right)} \\ \frac{1}{2}\sqrt{2 - \delta\mathbf{u} + 2\sqrt{2}\left(\frac{u_2}{r_0}\right)} - \frac{1}{2}\sqrt{2 - \delta\mathbf{u} - 2\sqrt{2}\left(\frac{u_2}{r_0}\right)} \end{pmatrix}$$

$$(4.7) \quad \mathbf{F}^{-1} \begin{pmatrix} z_1 \\ z_2 \end{pmatrix} = \begin{pmatrix} r_0 z_1 \sqrt{1 - \frac{1}{2}z_2^2} \\ r_0 z_2 \sqrt{1 - \frac{1}{2}z_1^2} \end{pmatrix}$$

where $\delta\mathbf{u} = \left(\frac{u_1}{r_0}\right)^2 - \left(\frac{u_2}{r_0}\right)^2$.

4.2. Bounds. Although the proposed schemes allow for arbitrary bounds to be placed on any system in question, the focus of this work is on hyperbolic systems of conservation laws. Judicious choices of the bounds allow for these schemes to enforce certain key properties of hyperbolic conservation laws (essentially) independently of the spatial discretization. We briefly present some examples of these bounds.

Remark 4.1 (Unbounded Constraints). If the admissible set of solutions is unbounded (i.e., $\mathcal{B} := (-\infty, \infty)^m$), the mapping function becomes a linear operator and the base RK scheme is recovered.

4.2.1. Positivity Preserving. A common constraint in hyperbolic systems is that \mathbf{u} (or some subset thereof) remains non-negative across the entire domain (e.g., density and total energy in the Euler equations, water height in the shallow water equations, etc.). Schemes that strictly enforce this condition, usually via the spatial discretization, are generally referred to as positivity preserving. This condition can be enforced through the bounds

$$(4.8) \quad \mathcal{B}_i(\mathbf{u}) := [0, \infty)^m \quad \forall i \in V.$$

4.2.2. Discrete Maximum Principle Satisfying. Enforcing the maximum principle property [12] at the discrete level is a feature that is beneficial to the application and analysis of numerical schemes as it is necessary for the unique entropy solution of scalar hyperbolic conservation laws to obey this property [2]. The formulation of these bounds is not necessarily unique and does have some dependency on the spatial discretization. For instance, one such definition can be

$$(4.9) \quad \mathbf{u}_i^{\min} = \min_{j \in \mathcal{A}(i)} \mathbf{u}_j, \quad \mathbf{u}_i^{\max} = \max_{j \in \mathcal{A}(i)} \mathbf{u}_j,$$

where $\mathcal{A}(i)$ is some domain of influence of point \mathbf{x}_i . A possible formulation of $\mathcal{A}(i)$ is the numerical domain of influence $\mathcal{I}(i)$ (i.e., the set of indices for which their associated shape function has support on \mathbf{x}_i) or some physical domain of influence related to the relative nodal spacing and propagation speed of the system (i.e., the direct Voronoi neighbors of \mathbf{x}_i). Stricter definitions for the bounds can draw on the works of Guermond et al. [6], Lax [12], Nessyahu and Tadmor [14] and utilize the direction of information propagation within the system (see [Subsection 4.2.4](#)). Regardless of the choice of the formulation, the bounds are then taken as such to enforce the discrete maximum principle.

$$(4.10) \quad \mathcal{B}_i(\mathbf{u}) := [\mathbf{u}_i^{\min}, \mathbf{u}_i^{\max}].$$

4.2.3. Entropy Dissipative. Let $\eta(\mathbf{u})$ be some convex entropy functional of (1.1). For entropy dissipative systems, if the condition

$$\frac{\partial}{\partial t} \int_{\mathcal{D}} \eta(\mathbf{u}) \leq 0$$

is not satisfied at least in a discrete sense, it may lead to solutions that are unphysical and qualitatively incorrect. To ensure that this property is not violated, the bounds can be formulated as

$$(4.11) \quad \mathcal{B}_i(\mathbf{u}) := \{\mathbf{u} \mid \eta(\mathbf{u}) \leq \eta_i^{\max}\},$$

where $\eta_i^{\max} \in \mathbb{R}$ is some maximum entropy. A discrete local entropy inequality can be enforced through a discrete maximum principle bound on the entropy functional, or, more strictly, through enforcing

$$(4.12) \quad \eta(\mathbf{u}_i^{n+1}) \leq \eta(\mathbf{u}_i^n) + \int_{t^n}^{t^{n+1}} \nabla \cdot \Sigma(\mathbf{u}_i) \, d\tau$$

for some entropy-flux pair (η, Σ) satisfying $\partial_{\mathbf{u}}\Sigma = \partial_{\mathbf{u}}\eta \partial_{\mathbf{u}}\mathbf{F}$.

To make the computation of the mapping function and its associated metrics tractable, it is beneficial for these terms to be algebraically defined to circumvent the need for iterative methods. For many convex functionals, identical constraints can be enforced through alternate formulations of the functional that are more amenable to algebraic transformations (see Guermond et al. [6] Sec. 7.5.2 and [Subsection 4.2.4](#)).

4.2.4. Invariant Domain Preserving. Invariant domain preserving schemes, introduced in Guermond and Popov [4], are shown to preserve any convex invariant of hyperbolic systems and satisfy the discrete entropy inequality for every admissible entropy of the system. These properties were achieved in Guermond and Popov [4] by using a graph-viscosity term to introduce a sufficient amount of artificial dissipation. By instead formulating the invariant domain as a set of admissible solutions, it is possible to enforce these properties via the BP-RK schemes.

For an in-depth overview of invariant sets and domains, the reader is referred to Guermond and Popov [4] and the works therein. In brief, a set is considered to be invariant with respect to (1.1) if for any pair of states within the set, the average of the entropy solution of the Riemann problem over the Riemann fan remains within that set. From the work of Hoff [8], it can be seen that this invariant set is convex for genuinely nonlinear hyperbolic equations. In general terms, a scheme is said to be invariant domain preserving if for some invariant set \mathcal{S} such that $\mathbf{u}_i^{n+1} \in \mathcal{S} \forall i \in V$, the temporal update of the scheme results in $\mathbf{u}_i^{n+1} \in \mathcal{S} \forall i \in V$.

The formulation of invariant domain preserving bounds is shown through the example of the compressible Euler equations, written in the form of (1.1) as

$$(4.13) \quad \mathbf{u} = \begin{bmatrix} \rho \\ \rho\mathbf{v} \\ E \end{bmatrix}, \quad \mathbf{F} = \begin{bmatrix} \rho\mathbf{v} \\ \rho\mathbf{v} \otimes \mathbf{v} + p\mathbf{I} \\ (E + p)\mathbf{v} \end{bmatrix},$$

where ρ is the density, $\rho\mathbf{v}$ is the momentum, E is the total energy, $p = (\gamma - 1)(E - \frac{1}{2}\rho\|\mathbf{v}\|_2^2)$ is the pressure, and $\gamma > 1$ is the ratio of specific heat capacities. The symbol \mathbf{I} denotes the identity matrix in $\mathbb{R}^{d \times d}$ and $\mathbf{v} = \rho\mathbf{v}/\rho$ denotes the velocity. From Guermond and Popov [4], the set

$$(4.14) \quad \mathcal{S} := \{(\rho, \rho\mathbf{v}, E) \mid \rho \geq 0, \epsilon(\mathbf{u}) \geq 0, \Psi(\mathbf{u}) \geq \Psi_0\}$$

is an invariant set for the Euler system for a specific internal energy $\epsilon(\mathbf{u}) := E/\rho - \frac{1}{2}\|\mathbf{v}\|_2^2$, specific physical entropy $\Psi(\mathbf{u})$ such that $-\Psi(\epsilon, \rho^{-1})$ is a strictly convex function, and any $\Psi_0 \in \mathbb{R}$.

Invariant domain preserving bounds can be enforced through discrete maximum principle bounds on the density,

$$(4.15) \quad \rho_{\min} \leq \rho \leq \rho_{\max},$$

and a local minimum condition on the specific physical entropy,

$$(4.16) \quad \Psi(\mathbf{u}) - \Psi_i^{\min} \geq 0, \quad \Psi(\mathbf{u}) = \frac{1}{\gamma - 1} \log(e\rho^{-\gamma}),$$

where $e = \rho\epsilon(\mathbf{u})$ denotes the internal energy. The minima/maxima are calculated through average Riemann solutions via the auxiliary states

$$(4.17) \quad \bar{\mathbf{U}}_{ij} = \frac{1}{2}(\mathbf{u}_i + \mathbf{u}_j) - \frac{\mathbf{c}_{ij}}{2\lambda_{\max}\|\mathbf{c}_{ij}\|_2}(\mathbf{F}(\mathbf{u}_j) - \mathbf{F}(\mathbf{u}_i)),$$

for $j \in \mathcal{A}(i)$ and some estimate of the maximum wavespeed of the system λ_{\max} .

From Guermond et al. [6], the entropy condition can be equivalently expressed as

$$(4.18) \quad e - \rho^\gamma \tilde{\Psi}_i^{\min} \geq 0, \quad \tilde{\Psi}(\mathbf{u}) := e\rho^{-\gamma} = \exp[(\gamma - 1)\Psi(\mathbf{u})],$$

which yields analytic transformations for the mapping function $\mathbf{G}(\mathbf{u})$. These constraints can be enforced through the general mappings presented in [Subsection 4.1](#) as

$$(4.19) \quad \rho \in [\rho_{\min}, \rho_{\max}],$$

$$(4.20) \quad \|\rho\mathbf{v}\|_2^2 \leq 2\rho(E - \rho^\gamma \tilde{\Psi}_i^{\min}),$$

$$(4.21) \quad E \geq \rho^\gamma \tilde{\Psi}_i^{\min} + \frac{1}{2}\rho^{-1}\|\rho\mathbf{v}\|_2^2.$$

Note that in contrast to the convex limiting approach of Guermond et al. [6], the mappings used to enforce these constraints have closed-form solutions and do not require the use of an iterative solver.

Remark 4.2 (Positivity Preserving Formulation). By instead setting $\tilde{\Psi}_i^{\min} = 0$, it is possible to recover a scheme that enforces positivity of density and pressure/internal energy independently of the entropy condition.

5. Implementation. The BP-RK schemes were implemented and utilized on a variety of hyperbolic problems, including nonlinear problems with discontinuities. To demonstrate the potential of these schemes, a pseudospectral method was used for the spatial discretization for solutions with discontinuous features without employing any explicit shock capturing approaches. The computational domain Ω is taken to be a periodic hypercube $[0, 1]^d$ (or an affine image thereof) with equispaced nodes $\{\mathbf{x}\}_{i \in V}$. The solution was approximated via a Fourier basis of degree $N - 1$ as

$$(5.1) \quad \mathbf{U}_h = \sum_{\|\mathbf{k}\|_\infty < N} \hat{\mathbf{u}}_k e^{2\pi i \mathbf{k} \cdot \mathbf{x} / N},$$

where $\mathbf{k} \in \mathbb{Z}^d$, $\mathbf{x} \in [0, 1]^d$, and $N \geq 1$. The projection of the nonlinear flux terms was evaluated via a pseudospectral (collocation) approach without anti-aliasing. BP-RK schemes of up to fourth order were considered in this work. These underlying RK schemes upon which the proposed methods were built are represented through the Butcher tableaux in [Figure 1](#).

0		0		0		0	
$\frac{1}{2}$	$\frac{1}{2}$	$\frac{1}{3}$	$\frac{1}{3}$	$\frac{1}{2}$	0	$\frac{1}{2}$	$\frac{1}{2}$
	0	$\frac{2}{3}$	0	1	0	0	1
		$\frac{1}{4}$	0	$\frac{1}{6}$	$\frac{1}{3}$	$\frac{1}{3}$	$\frac{1}{6}$
	1	$\frac{3}{4}$	$\frac{3}{4}$				

We consider two formulations for the bounds: discrete maximum principle (DMP) for scalar-valued solutions and invariant domain preserving (IDP) for vector-valued solutions. For both of these methods, the support $\mathcal{A}(i)$ at a point \mathbf{x}_i is taken to be the set of direct Voronoi neighbors of \mathbf{x}_i , including \mathbf{x}_i itself. The calculation of the maximum wavespeed for the auxiliary states in the IDP approach was performed using an exact Gudonov-type Riemann solver [18].

6. Results.

6.1. Linear Transport. The convergence rates and bounds-preserving properties of the BP-RK schemes were tested on the linear transport equation in one dimension:

$$(6.1) \quad \partial_t u + \partial_x(cu) = 0.$$

The transport velocity was set as $c = 1$ and the domain was set as $\Omega = [0, 1]$ with periodic boundary conditions. A smooth sinusoidal initial condition, given as

$$(6.2) \quad u_0(x) = \sin(2\pi x),$$

was used to validate the results of [Theorem 3.5](#). The L^2 norm of the solution error, defined as

$$(6.3) \quad \|e\|_2 = \sqrt{\sum_{i=0}^{N-1} h(u_i - u_0(x_i))^2},$$

with $h = 1/N$, was computed at $t = 100$, corresponding to 100 traverses through the domain. The convergence rate of the L^2 error with respect to Δt for a pseudospectral spatial discretization with $N = 32$ using RK and BP-RK temporal integration with DMP bounds is shown in [Figure 2](#) and tabulated in [Table 1](#). The BP-RK schemes recovered the theoretical convergence rates of the underlying RK schemes, as stated by [Theorem 3.5](#), albeit with larger leading error constants for $p > 1$. These effects may be attributed to the larger impact of numerical precision errors due to the nonlinear transformations required by the BP-RK schemes.

Order	RK	BP-RK
1	1.004	1.005
2	2.000	2.000
3	2.999	3.002
4	3.674	3.959

Table 1: Convergence rates of the L^2 norm of the error with respect to time step using Runge-Kutta and bounds preserving Runge-Kutta temporal integration.

The ability of the BP-RK schemes to enforce bounds was initially evaluated for a linear transport problem with a non-smooth initial condition given by

$$(6.4) \quad u_0(x) = \begin{cases} \exp(-300(2x - 0.3)^2), & \text{if } |2x - 0.3| \leq 0.25, \\ 1, & \text{if } |2x - 0.9| \leq 0.2, \\ \sqrt{1 - \left(\frac{2x-1.6}{0.2}\right)^2}, & \text{if } |2x - 1.6| \leq 0.2, \\ 0, & \text{else.} \end{cases}$$

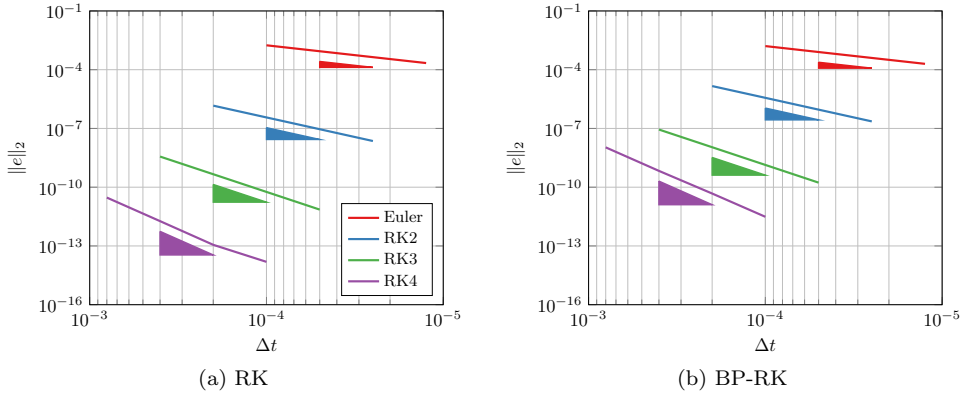


Fig. 2: Convergence of the L^2 norm of the error with respect to time step using Runge-Kutta (left) and bounds preserving Runge-Kutta temporal integration (right). Solid triangles represent the theoretical convergence rates.

The solution at $t = 100$ using a pseudospectral discretization with $N = 128, 256$

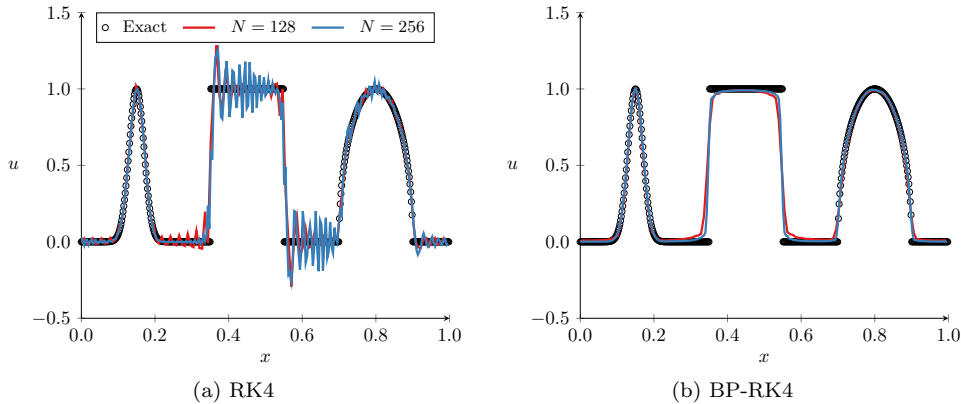


Fig. 3: Solution of the linear transport equation at $t = 100$ using RK4 (left) and bounds preserving RK4 temporal integration (right), pseudospectral spatial discretization ($N = 128, 256$), and discrete maximum principle bounds.

is shown in Figure 3 for RK4 and BP-RK4 temporal integration with DMP bounds. Without the BP-RK schemes, the solution was highly oscillatory with significant overshoots and undershoots around discontinuous features. When the BP-RK4 was used, the predicted solution was in excellent agreement with the exact solution, and no spurious oscillations were observed. Due to the enforcement of the discrete maximum principle, the solution remained within the range of the initial conditions.

6.2. Nonlinear Transport. The BP-RK schemes were then evaluated for nonlinear hyperbolic conservation laws that develop discontinuities from smooth initial

conditions. The inviscid Burgers equation in one-dimension, given by

$$(6.5) \quad \partial_t u + \partial_x \left(\frac{1}{2} u^2 \right) = 0,$$

with the initial conditions

$$(6.6) \quad u_0(x) = \sin(2\pi x) + 2,$$

was solved on the periodic domain $\Omega = [0, 1]$ using a pseudospectral spatial discretization with $N = 64$. The computed solution at $t = 1$ is shown in Figure 4 using RK2

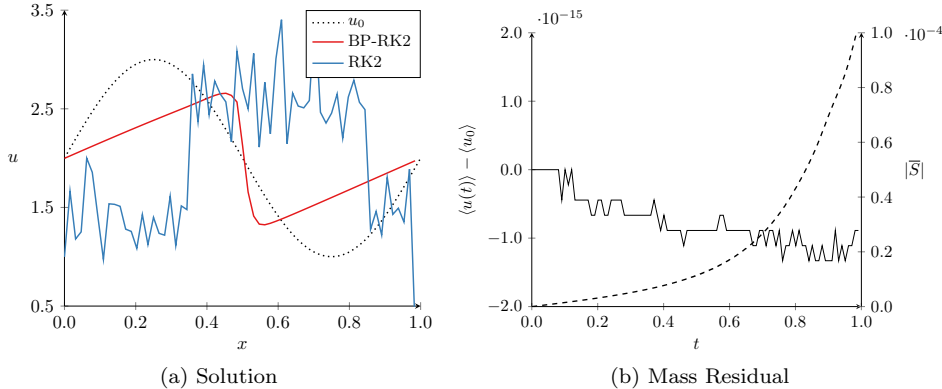


Fig. 4: *Left*: Solution of the Burgers equation at $t = 1$ using RK2 and bounds preserving RK2 temporal integration, pseudospectral spatial discretization ($N = 64$), and discrete maximum principle bounds. *Right*: Space-integrated mass residual (solid) and magnitude of \bar{S} (dashed) over time.

and BP-RK2 temporal integration with DMP bounds. Without the BP-RK schemes, the presence of Gibbs phenomena compounded with the nonlinearities in the transport equation made the results unusable for practical purposes due to their highly oscillatory nature. With the BP-RK2 scheme and DMP bounds, the solution remained well-behaved even as discontinuities became present in the solution through the introduction of an adequate amount of numerical dissipation around the shock via the temporal scheme. Figure 4 additionally shows the space-integrated mass of the solution, $\langle u(t) \rangle = \sum_{i \in V} m_i u_i(t)$, and the magnitude of the \bar{S} term with respect to time. The scheme conserved mass down to numerical precision, as expected by Theorem 3.7. The effect of the BP-RK2 scheme in enforcing the bounds is represented through the magnitude of the \bar{S} term, as larger values of \bar{S} indicate larger deviations from the underlying RK scheme. The magnitude of \bar{S} was initially low as the solution was smooth and therefore the mappings were approximately linear, but as the solution began to develop a discontinuity, the magnitude increased to compensate for the mass defect due to the nonlinearities in the mapping functions. However, even at its maximum, this defect was still orders of magnitude lower than the overall mass of the system.

6.3. Euler Equations. The assessment of the BP-RK schemes was extended to vector-valued solutions and to higher-dimensions through the Euler equations, as presented in (4.13). For brevity, we express the solution in terms of the primitive variables $\mathbf{q} = [\rho, \mathbf{v}, P]^T$.

6.3.1. Sod Shock Tube. The Sod shock tube problem [17] was used to evaluate the ability of the proposed scheme to predict the three main features of Riemann problems: expansion fans, contact discontinuities, and shock waves. The problem is defined on the domain $\Omega = [0, 1]$ with the initial conditions

$$(6.7) \quad \mathbf{q}_0(x) = \begin{cases} \mathbf{q}_l, & \text{if } x \leq 0.5, \\ \mathbf{q}_r, & \text{else,} \end{cases} \quad \text{given } \mathbf{q}_l = \begin{bmatrix} 1 \\ 0 \\ 1 \end{bmatrix}, \quad \mathbf{q}_r = \begin{bmatrix} 0.125 \\ 0 \\ 0.1 \end{bmatrix}.$$

The problem was periodized by extending the domain to $\Omega = [-1, 1]$ and reflecting the initial conditions about $x = 0$. The resolution of the spatial scheme N is presented in terms of the half-domain. The density profile of the solution at $t = 0.2$ using BP-RK4 temporal integration, pseudospectral spatial discretization ($N = 128, 256$), and invariant domain preserving bounds is shown in Figure 5. Given the coarse resolution ($N = 128$), the results were in excellent agreement with the exact solution, showing no observable spurious oscillations and good resolution of the contact discontinuity, shock wave, and expansion fan without any explicit shock capturing approaches. When the resolution was increased ($N = 256$), even better agreement was observed, with particularly notable improvements at the front of the expansion fan and the contact discontinuity. Without the BP-RK scheme, the solution diverged due to the spurious oscillations causing negative density and pressure values.

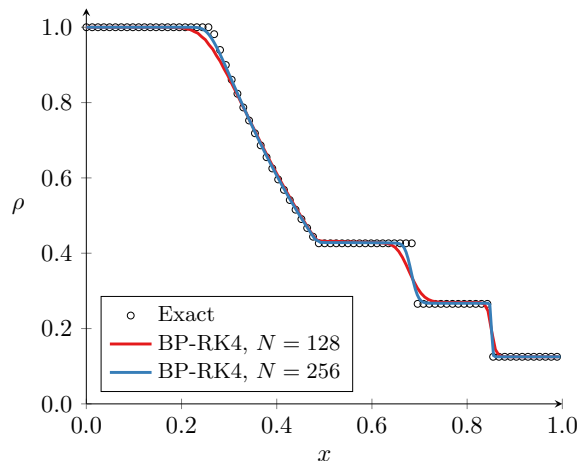


Fig. 5: Density profile of the Sod shock tube at $t = 0.2$ using bounds preserving RK4 temporal integration, pseudospectral spatial discretization ($N = 128, 256$), and invariant domain preserving bounds.

6.3.2. 2D Riemann Problem. For the extension to higher-dimensions, a two-dimensional Riemann problem was considered, introduced as case 12 in Liska and Wendroff [13]. The problem is defined on the domain $\Omega = [0, 1]^2$ with the initial conditions given in Figure 6. Similarly to the Sod shock tube, the domain is periodized by reflecting the domain about the $x = 0$ and $y = 0$ axes. The contours of density computed using BP-RK4 temporal integration, pseudospectral spatial discretization ($N = 400^2$), and invariant domain preserving bounds are shown Figure 7. The results are in good agreement with the various methods in Liska and Wendroff [13], with good

resolution of the contact discontinuities and shock fronts and no observable spurious oscillations. A comparison with the results of a pseudospectral spatial discretization using an entropy viscosity approach from Guermond et al. [5] is also shown in Figure 7. Comparable results were seen with the BP-RK scheme even with a lower resolution and without an explicit shock-capturing approach.

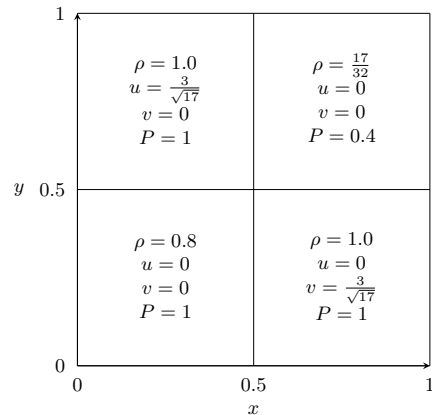


Fig. 6: Initial conditions for the 2D Riemann problem on the subdomain $\Omega = [0, 1]^2$.

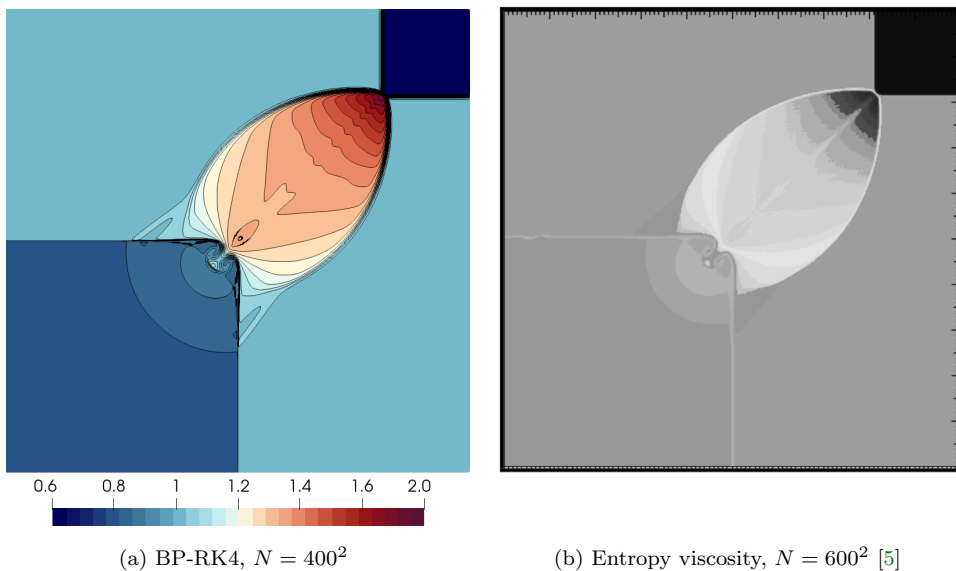


Fig. 7: Contours of density for the 2D Riemann problem at $t = 0.2$. *Left*: Bounds preserving RK4 temporal integration, pseudospectral spatial discretization ($N = 400^2$), and invariant domain preserving bounds. *Right*: Pseudospectral spatial discretization ($N = 600^2$) with entropy viscosity (Guermond et al. [5]).

7. Conclusion. In this work, we introduced bounds preserving RK (BP-RK) schemes, a novel formulation of explicit RK temporal integration schemes that preserve any locally-defined quasiconvex set of bounds for the solution. These schemes operate on the basis of a nonlinear, bijective mapping between an admissible quasiconvex set of solutions and the real domain prior to temporal integration which is followed by an inverse mapping. The proposed techniques are generally applicable to a wide variety of problems, but the emphasis in this work was on nonlinear hyperbolic conservation laws, for which it was shown that an assortment of methods, such as positivity preserving, discrete maximum principle satisfying, entropy dissipative, and invariant domain preserving schemes, could be recovered essentially independently of the spatial discretization. It was also shown, both analytically and experimentally, that the BP-RK schemes preserve any linear invariant of the system and recover the order of accuracy of the underlying RK schemes upon which they are built. For many applications, the additional cost of the proposed schemes is almost negligible – simply the evaluation of two mappings with closed-form solutions. To show the utility of these schemes, the results of the computation of nonlinear hyperbolic conservation laws with discontinuous solutions using a pseudospectral method without an explicit shock capturing approach were presented. Even though the spatial discretization scheme was ill-suited for discontinuous problems, the results of the BP-RK were on par with dedicated shock capturing schemes, showing good resolution of discontinuous features without any observable spurious oscillations. For general applications for which the spatial discretization schemes are better suited for the problems at hand, BP-RK schemes can potentially offer superior performance at a lower computational cost than dedicated spatial discretization schemes and allow for generalizability between various constraints without the need to derive and implement new discretizations.

References.

- [1] M. Calvo, D. Hernández-Abreu, J. I. Montijano, and L. Rández. On the preservation of invariants by explicit Runge–Kutta methods. *SIAM Journal on Scientific Computing*, 28(3):868–885, January 2006. doi: 10.1137/04061979x.
- [2] Constantine M. Dafermos. *Hyperbolic Conservation Laws in Continuum Physics*, chapter 9, pages 271–324. Springer Berlin Heidelberg, 2010. doi: 10.1007/978-3-642-04048-1.
- [3] Hermano Frid. Maps of convex sets and invariant regions for finite-difference systems of conservation laws. *Archive for Rational Mechanics and Analysis*, 160(3):245–269, November 2001. doi: 10.1007/s002050100166.
- [4] Jean-Luc Guermond and Bojan Popov. Invariant domains and first-order continuous finite element approximation for hyperbolic systems. *SIAM Journal on Numerical Analysis*, 54(4):2466–2489, January 2016. doi: 10.1137/16m1074291.
- [5] Jean-Luc Guermond, Richard Pasquetti, and Bojan Popov. Entropy viscosity method for nonlinear conservation laws. *Journal of Computational Physics*, 230(11):4248–4267, May 2011. doi: 10.1016/j.jcp.2010.11.043.
- [6] Jean-Luc Guermond, Bojan Popov, and Ignacio Tomas. Invariant domain preserving discretization-independent schemes and convex limiting for hyperbolic systems. *Computer Methods in Applied Mechanics and Engineering*, 347:143–175, April 2019. doi: 10.1016/j.cma.2018.11.036.
- [7] Ernst Hairer, Gerhard Wanner, and Christian Lubich. *Geometric Numerical Integration: Structure-Preserving Algorithms for Ordinary Differential Equations*. Springer-Verlag, 2006. doi: 10.1007/3-540-30666-8.
- [8] David Hoff. Invariant regions for systems of conservation laws. *Transactions*

- of the American Mathematical Society*, 289(2):591–591, February 1985. doi: 10.1090/s0002-9947-1985-0784005-3.
- [9] Arieh Iserles and Antonella Zanna. Preserving algebraic invariants with runge–kutta methods. *Journal of Computational and Applied Mathematics*, 125(1-2):69–81, December 2000. doi: 10.1016/s0377-0427(00)00459-3.
 - [10] A. Jameson, W. Schmidt, and E. Turkel. Numerical solution of the Euler equations by finite volume methods using Runge–Kutta time stepping schemes. In *14th Fluid and Plasma Dynamics Conference*. American Institute of Aeronautics and Astronautics, June 1981. doi: 10.2514/6.1981-1259.
 - [11] David I. Ketcheson. Relaxation Runge–Kutta methods: Conservation and stability for inner-product norms. *SIAM Journal on Numerical Analysis*, 57(6):2850–2870, January 2019. doi: 10.1137/19m1263662.
 - [12] Peter D. Lax. Weak solutions of nonlinear hyperbolic equations and their numerical computation. *Communications on Pure and Applied Mathematics*, 7(1):159–193, February 1954. doi: 10.1002/cpa.3160070112.
 - [13] Richard Liska and Burton Wendroff. Comparison of several difference schemes on 1D and 2D test problems for the Euler equations. *SIAM Journal on Scientific Computing*, 25(3):995–1017, January 2003. doi: 10.1137/s1064827502402120.
 - [14] Haim Nessyahu and Eitan Tadmor. Non-oscillatory central differencing for hyperbolic conservation laws. *Journal of Computational Physics*, 87(2):408–463, April 1990. doi: 10.1016/0021-9991(90)90260-8.
 - [15] Hendrik Ranocha, Mohammed Sayyari, Lisandro Dalcin, Matteo Parsani, and David I. Ketcheson. Relaxation Runge–Kutta methods: Fully discrete explicit entropy-stable schemes for the compressible Euler and Navier–Stokes equations. *SIAM Journal on Scientific Computing*, 42(2):A612–A638, January 2020. doi: 10.1137/19m1263480.
 - [16] Chi-Wang Shu. Bound-preserving high-order schemes for hyperbolic equations: Survey and recent developments. In *Theory, Numerics and Applications of Hyperbolic Problems II*, pages 591–603. Springer International Publishing, 2018. doi: 10.1007/978-3-319-91548-7_44.
 - [17] Gary A Sod. A survey of several finite difference methods for systems of nonlinear hyperbolic conservation laws. *Journal of Computational Physics*, 27(1):1–31, April 1978. doi: 10.1016/0021-9991(78)90023-2.
 - [18] Eleuterio F. Toro. The Riemann problem for the Euler equations. In *Riemann Solvers and Numerical Methods for Fluid Dynamics*, chapter 4, pages 115–157. Springer Berlin Heidelberg, 1997. doi: 10.1007/978-3-662-03490-3_4.